ELSEVIER

Journal of Wind Engineering
and Industrial Aerodynamics 89 (2001) 1335–1350

JOURNAL OF wind engineering AND industrial aerodynamics

www.elsevier.com/locate/jweia

Nonlinear response analysis of long-span bridges under turbulent winds

Xinzhong Chen*, Ahsan Kareem

Department of Civil Engineering and Geological Sciences, University of Notre Dame, USA

Abstract

This paper presents a time domain analysis framework for predicting nonlinear response of long-span bridges under turbulent winds. The nonlinear unsteady aerodynamic forces are modeled based on static force coefficients, flutter derivatives, admittance functions, and their spanwise correlations at varying angles of incidence. This analysis framework incorporates frequency dependent parameters of unsteady aerodynamic forces by utilizing a rational function approximation technique. A comparison with conventional linear approach is made through response analysis of a long-span suspension bridge. The effects of turbulence on the flutter instability are also addressed.

Keywords: Flutter; Buffeting; Bridge; Aerodynamics; Aeroelastic analysis; Nonlinear analysis; Turbulence; Wind

1. Introduction

Analytical prediction of wind induced buffeting response and flutter instability have predominantly been conducted in the frequency domain in which the aerodynamic forces are linearized at the mean displaced position (e.g. Refs. [1,2]). The frequency domain approach is in general limited to linear structures excited by stationary wind loads. A time domain framework was proposed by Chen et al. [3], incorporating the frequency dependent characteristics of aerodynamic forces that are often neglected in current time domain analyses due to modeling difficulty (e.g., Ref. [4]). Central to this approach is the rational function approximation of the frequency dependent characteristics of self-excited and buffeting forces. A

*Corresponding author. Tel.: +1-219-631-5380; fax: +1-219-631-9236.
E-mail address: xchen@nd.edu (X. Chen).

0167-6105/01/$ - see front matter
PII: S0167-6105(01)00147-7

state-space model approach has also been presented by Chen and Kareem [5], in which the response of bridges under turbulent winds has been taken as the output of an integrated system driven by a vector-valued white noise. With this state-space model approach, the buffeting response can be directly calculated by using Lyapunov equation instead of using conventional spectral analysis for computational efficiency, and aerodynamic force information can be readily considered in a structural control design as a feed-forward link with the potential to enhance the control effectiveness.

Experimental wind tunnel studies have indicated that turbulence can both stabilize and destabilize the flutter instability depending on the geometric configuration of bridge sections and the characteristics of wind fluctuations (e.g., Refs. [6,7]). A number of analytical studies using stochastic approaches by randomizing the dynamic pressure have been conducted to predict some general changes in flutter instability due to turbulence (e.g., Ref. [8]). Scanlan [9] addressed the potential mechanism of turbulence on the single torsional flutter due to the spanwise correlation loss of the self-excited forces. Experimental measurements using a rectangular section have indicated that while turbulence results in a slight loss of the spanwise correlation of the self-excited forces, the correlation remains quite close to unity [10]. Further experimental investigation of this issue needs to be conducted including pressure measurements with large spanwise separation. Diana et al. [11] have analytically investigated the effects of turbulence on flutter using a nonlinear aerodynamic force model which is based on the so-called "quasi-static corrected theory". This nonlinear force model incorporated frequency dependent characteristics by decomposing the total response into components with different frequencies.

Aerodynamic force parameters of bridge decks are generally highly sensitive to the angle of incidence (e.g., Ref. [12]). Even for small level of turbulence, the effective angle of incidence due to structural motions and wind fluctuations may vary to a level such that the nonlinearity of aerodynamic force may not be neglected. This paper emphasizes the dependence of aerodynamic force parameters on the angle of incidence and its influences on the buffeting and flutter responses of bridges. A novel time domain framework for predicting the buffeting and flutter responses is presented incorporating the aerodynamic nonlinearities and frequency dependency due to the aerodynamic memory effects. A comparison with the conventional linear approach is made through response analysis of a long-span suspension bridge.

2. Linear aerodynamic forces

Traditional linear aerodynamic force model assumes that the variation of effective angle of incidence is small enough that aerodynamic forces can be linearized at the statically deformed position and that the variation of aerodynamic parameters is negligible. The linear aerodynamic forces, i.e., lift (downward), drag (downwind) and pitching moment (nose-up) are commonly separated into mean averaged, self-excited and buffeting force components. The mean averaged (static) wind forces acting on an

element of length l are expressed as

$$L_s = -\frac{1}{2}\rho U^2 lBC_L(\alpha_s); \quad D_s = \frac{1}{2}\rho U^2 lBC_D(\alpha_s); \quad M_s = \frac{1}{2}\rho U^2 lB^2 C_M(\alpha_s), \tag{1}$$

where ρ is the air density; U is the mean wind velocity; $B = 2b$ is the bridge deck width; C_L, C_D and C_M are the mean lift, drag and pitching moment coefficients, respectively; and α_s is the time-averaged (static) angle of the bridge section.

The time-varying self-excited forces resulting from the structural motions can be expressed as the sum of components associated with each structural motion component in vertical, lateral and torsional directions. These are functions of its frequency of oscillation due to the unsteady aerodynamic memory effects, and can be represented in terms of convolution integrals involving impulse response functions (e.g., Refs. [3,13]). Assuming the self-excited forces are spatially fully correlated, for example, the pitching moment component is given by

$$M_{se}(t) = \frac{1}{2}\rho U^2 l \int_{-\infty}^{t} (I_{Mh}(\alpha_s, t-\tau)h(\tau) + I_{Mp}(\alpha_s, t-\tau)p(\tau) + I_{M\alpha}(\alpha_s, t-\tau)\alpha(\tau))\,d\tau, \tag{2}$$

where h, p and α are the vertical, lateral and torsional displacement, respectively; I_{Mh}, I_{Mp} and $I_{M\alpha}$ are the aerodynamic impulse response functions representing the influence of motions at a certain moment in time on the generation of self-excited forces for a period of time. Analogous formulations hold for the lift and drag components.

Similarly, the buffeting forces can be expressed as the sum of components associated with horizontal and vertical wind fluctuations (u and w) in terms of impulse response functions [3,13,14]. Taking into account the spanwise correlation of the buffeting forces, for example, the moment component is given by

$$M_b(t) = \frac{1}{2}\rho U^2 l \int_{-\infty}^{t} \int_{-\infty}^{\tau_2} \left(J_{Mu}(\alpha_s, t-\tau_2) I_{Mu}(\alpha_s, \tau_2-\tau_1) \frac{u(\tau_1)}{U} + J_{Mw}(\alpha_s, t-\tau_2) I_{Mw}(\alpha_s, \tau_2-\tau_1) \frac{w(\tau_1)}{U} \right) d\tau_1\, d\tau_2, \tag{3}$$

where I_{Mu} and I_{Mw} are the aerodynamic impulse response functions of buffeting forces representing the aerodynamic memory effects of buffeting forces per unit length; and J_{Mu} and J_{Mw} indicate the impulse response functions representing the spatial correlation characteristics. Analogous formulations hold for the lift and drag components.

Direct determination of these impulse response functions for bluff bridge sections is not without difficulty, and the associated technique based on wind tunnel tests have not been well established. Instead, the techniques for identifying the frequency domain aerodynamic force parameters such as flutter derivatives, admittance functions and spanwise coherence have been extensively developed, and rich data for various geometric configurations of bridge sections has been accumulated. Therefore, these impulse response functions defined in time domain can be quantified through their relationship to the unsteady force parameters defined in frequency

domain. For example, the torsional motion induced pitching moment $M_{se\alpha}(t)$ is given in terms of the flutter derivatives A_2^* and A_3^* in the frequency domain as

$$M_{se\alpha}(t) = \frac{1}{2}\rho U^2 l(2b^2)\left[kA_2^*(k)\frac{b\dot{\alpha}}{U} + k^2 A_3^*(k)\alpha\right], \tag{4}$$

where $k = \omega b/U$ is the reduced frequency.

The relationship between $\bar{I}_{M\alpha}(k)$, $A_2^*(k)$ and $A_3^*(k)$ is

$$\bar{I}_{M\alpha}(k) = 4b^2 C'_M C_{M\alpha} = 2k^2 b^2[A_3^*(k) + \mathrm{i}A_2^*(k)], \tag{5}$$

where $C'_M = \mathrm{d}C_M/\mathrm{d}\alpha$; and the over bar indicates the Fourier transform.

Similarly, the buffeting force component $M_{bw}(t)$ is expressed in terms of admittance function $\chi_{Mw}(k)$ and joint acceptance $\bar{J}_{Mw}(k)$ as

$$M_{bw}(t) = \frac{1}{2}\rho U^2 l B^2 C'_M \chi_{Mw}(k)\bar{J}_{Mw}(k)\frac{w(t)}{U}, \tag{6}$$

where the joint acceptance function is given in terms of the coherence function coh_{Mw} as

$$\bar{J}^2_{Mw}(k) = \frac{1}{l^2}\int_0^l \int_0^l coh_{Mw}(x_1, x_2; f)\,\mathrm{d}x_1\,\mathrm{d}x_2, \tag{7}$$

where x_1 and x_2 are the spatial coordinates.

The relationship between $\bar{I}_{Mw}(k)$ and $\chi_{bw}(k)$ is

$$\bar{I}_{Mw}(k) = 4b^2 C'_M \chi_{Mw}(k) \tag{8}$$

and the impulse response functions representing the spanwise correlation of buffeting forces are given by the inverse Fourier transform of the joint acceptance functions.

3. Rational function approximation

Since the frequency domain force parameters are normally known only at limited number of discrete values of the reduced frequency k, it is difficult to directly use the aforementioned relationships (Eqs. (5) and (8)) through an inverse Fourier transform to quantify the impulse response functions. Therefore, approximate continuous functions of the reduced frequency are required for describing frequency dependent aerodynamic force parameters for future analysis. The rational function approximation technique can be utilized for this content (e.g., Refs. [2,3,8,15]). For the self-excited forces, the aerodynamic transfer functions between forces and structural motions, for example of $M_{se\alpha}$, can be approximated in terms of the following rational function:

$$2k^2 b^2(A_3^* + \mathrm{i}A_2^*) = A_{M\alpha,1} + (\mathrm{i}k)A_{M\alpha,2} + (\mathrm{i}k)^2 A_{M\alpha,3} + \sum_{j=1}^{m_{M\alpha}} \frac{(\mathrm{i}k)A_{M\alpha,j+3}}{\mathrm{i}k + d_{M\alpha,j}}, \tag{9}$$

where $A_{M\alpha,1}$, $A_{M\alpha,2}$, $A_{M\alpha,3}$, $A_{M\alpha,j+3}$ and $d_{M\alpha,j}$ $(d_{M\alpha,j} \geqslant 0;\ j = 1, \ldots, m_{M\alpha})$ are frequency independent coefficients that can be determined by fitting the

experimentally obtained flutter derivatives at different reduced frequencies in a least square sense.

Accordingly, the unsteady self-excited force $M_{se\alpha}$ is given in the time domain as

$$M_{se\alpha}(t) = \frac{1}{2}\rho U^2 l\left[A_{M\alpha,1}\alpha(t) + A_{M\alpha,2}\frac{b}{U}\dot{\alpha}(t) + A_{M\alpha,3}\frac{b^2}{U^2}\ddot{\alpha}(t) + \sum_{j=1}^{m_{M\alpha}}\phi_{M\alpha,j}(t)\right], \quad (10)$$

$$\dot{\phi}_{M\alpha,j}(t) = -\frac{d_{M\alpha,j}U}{b}\phi_{M\alpha,j}(t) + A_{M\alpha,j+3}\dot{\alpha}(t), \quad (11)$$

where $\phi_{M\alpha,j}(t)$ $(j = 1 \sim m_{M\alpha})$ are the augmented aerodynamic states.

Similar formulations can be obtained for buffeting forces [3]. Generally, the aerodynamic transfer functions in terms of flutter derivatives, admittance and joint acceptance functions can be expressed as the following rational function with negative poles, indicating that the forces lag the body motions or incoming wind fluctuations:

$$H(k) = \frac{N(\mathrm{i}k)}{D(\mathrm{i}k)} = \frac{b_0(\mathrm{i}k)^n + b_1(\mathrm{i}k)^{n-1} + \cdots + b_n}{(\mathrm{i}k)^n + a_1(\mathrm{i}k)^{n-1} + \cdots + a_n}. \quad (12)$$

The coefficients $a_1, \ldots, a_n$ and $b_1, \ldots, b_n$ can be evaluated by minimizing the error

$$\sum_{j=1}^{m}\left[H(k_j) - \frac{N(\mathrm{i}k_j)}{D(\mathrm{i}k_j)}\right]^2, \quad (13)$$

where $H(k_j)$ $(j = 1, \ldots, m)$ are measured aerodynamic transfer function data.

Once these aerodynamic transfer functions have been expressed in terms of rational function format, the frequency dependent aerodynamic forces can be calculated through a set of linear differential equations or through a state-space model [5]. It is noted that if the frequency-dependent aerodynamic force parameters can be represented exactly or with an acceptable error by the rational functions of reduced frequency, formulations in the time domain would lead to a rigorous interpretation of these parameters defined in the frequency domain. Most time domain analysis approaches utilize quasi-steady aerodynamic force model due to the difficulty in modeling frequency dependent force parameters in time domain. This quasi-steady force model can take into account the nonlinear dependence of forces on the effective angle of incidence, while the definition of the effective angle of incidence is questionable. The disadvantage of quasi-steady force model is that the unsteady fluid memory effect that results in the aerodynamic forces to be frequency dependent cannot be described, and therefore it is only applicable at very high reduced velocity. Using the frequency domain force parameters and the rational function approximation technique leads to an accurate estimate of unsteady forces and attendant response of bridges in the time domain over those based on frequency independent quasi-steady assumption. Similar applications of the rational function approximation technique can be found in the engineering problems such as soil-structure and wave-structure interactions.

4. Nonlinear aerodynamic forces

For bridge sections with aerodynamic forces that are highly sensitive to the angle of incidence, nonlinearities in aerodynamic forces may not be neglected. These nonlinearities arise from the dependence of aerodynamic forces on the instantaneous effective angle of incidence, which consists of the contribution of wind fluctuations and the static and dynamic structural motions.

Following the formulation used for static and quasi-static forces, the nonlinear aerodynamic forces can be generally expressed as functions of the effective angle of incidence α_e with properly defined force coefficients. The effective angle of incidence can be further separated into low-frequency (large scale) and high-frequency (small scale) components corresponding to the frequencies lower than and higher than a critical frequency, e.g., the lowest natural frequency of the bridge, i.e.

$$\alpha_e(t) = \alpha_e^l(t) + \alpha_e^h(t), \tag{14}$$

where superscripts l and h indicate the low- (including static component) and high-frequency components.

Accordingly, the nonlinear aerodynamic forces are separated into corresponding low- and high-frequency components. The low-frequency component is modeled as a nonlinear function of the effective angle $\alpha_e^l(t)$, and the high-frequency component is linearized at $\alpha_e^l(t)$ and further separated into self-excited and buffeting force components as follows:

$$\mathbf{F} = \mathbf{F}(\alpha_e) = \mathbf{F}(\alpha_e^l) + \frac{d\mathbf{F}}{d\alpha}\alpha_e^h = \mathbf{F}^l + \mathbf{F}_{se}^h + \mathbf{F}_b^h. \tag{15}$$

The low-frequency components of aerodynamic forces can be expressed using the quasi-steady theory due to high value of the reduced velocity as the following nonlinear form (including static components):

$$L^l = F_L^l \cos\phi^l - F_D^l \sin\phi^l; \quad D^l = F_L^l \sin\phi^l + F_D^l \cos\phi^l; \quad M^l = F_M^l, \tag{16}$$

$$F_L^l = -\frac{1}{2}\rho V_r^2 B l C_L(\alpha_e^l); \quad F_D^l = \frac{1}{2}\rho V_r^2 B l C_D(\alpha_e^l); \quad F_M^l = \frac{1}{2}\rho V_r^2 B^2 l C_M(\alpha_e^l), \tag{17}$$

$$V_r^2 = (U + u^l - \dot{p}^l)^2 + (w^l + \dot{h}^l + b_1\dot{\alpha}^l)^2, \tag{18}$$

$$\alpha_e^l = \alpha_s + \phi^l; \quad \phi^l = \arctan\left(\frac{w^l + \dot{h}^l + b_1\dot{\alpha}^l}{U + u^l - \dot{p}^l}\right), \tag{19}$$

where b_1 is assumed as $b/2$.

When the low-frequency dynamic response is comparatively small and negligible as is the case for most long-span bridges, α_e^l is simplified as

$$\alpha_e^l = \alpha_s + \arctan\left(\frac{w_l}{U + u_l}\right). \tag{20}$$

The linearized high-frequency components of aerodynamic forces, for example, the moment components of self-excited and buffeting forces are given by

$$M^h_{se\alpha}(t) = \frac{1}{2}\rho U^2 l \int_{-\infty}^{t} I_{M\alpha}(\alpha^l_e, t-\tau)\alpha^h(\tau)\,d\tau, \tag{21}$$

$$M^h_{bw}(t) = \frac{1}{2}\rho U^2 l \int_{-\infty}^{t}\int_{-\infty}^{\tau_2} J_{Mw}(\alpha^l_e, t-\tau_2) I_{Mw}(\alpha^l_e, \tau_2-\tau_1)\frac{w^h(\tau_1)}{U}\,d\tau_1\,d\tau_2. \tag{22}$$

By using the rational function approximation technique to express the frequency domain force parameters as a functions of reduced velocity at varying angles of incidence, the aerodynamic impulse response functions and hence the time histories of nonlinear unsteady aerodynamic forces can be calculated in time domain. It is noted that the difference between linear and nonlinear analysis is that in nonlinear analysis the aerodynamic force parameters are modulated by the instantaneous low-frequency effective angle of incidence $\alpha^l_e(t)$, while in the traditional linear analysis the force parameters take the values at the statically deformed position of bridge sections.

Diana et al. [11] also proposed a nonlinear aerodynamic force model based on the so-called "quasi-steady corrected theory". This model decomposed the total response into components with different frequencies, and the frequency dependent force characteristics at the corresponding frequencies were utilized to capture the unsteady feature of the aerodynamic forces. In this study as mentioned above, the nonlinear force mode is based on the static force coefficients, flutter derivatives and admittance functions along with spanwise coherence at varying angles of incidence, and has a clear linkage with the conventional linear force model (e.g., Ref. [13]). In addition, the unsteady feature of the aerodynamic forces is modeled by using the rational function approximation technique with inherent advanced computational efficiency.

5. Solution of equations of motion

A time domain response analysis requires input spatio-temporal random time histories of wind fluctuations. The simulation of stationary Gaussian wind fluctuations can be accomplished using spectral, time series and other techniques (e.g., Ref. [16]). In this study, a multi-variate auto-regressive (AR) scheme is utilized for simulating the time histories of wind fluctuations at the center of each bridge element with prescribed auto-spectral and cross-spectral characteristics [3]. The power spectral density (PSD) components of the **u** and **w** vectors used herein are given by the von Kármán spectra. Using the simulated wind fluctuations at the center of each element, the low- and high-frequency components of wind fluctuations can be extracted using fast Fourier transform (FFT) and inverse fast Fourier transform (IFFT) calculations.

The dynamic response is calculated by using the Newmark Beta step-by-step integration scheme. An iterative calculation procedure is necessary for treating both

the low- and high-frequency components of response. At each time step and for each element the effective angle of incidence $\alpha_e^l(t)$ is calculated and the associated aerodynamic parameters are then determined for the calculation of the linear high-frequency force component. For most long span bridges, the low-frequency dynamic response is negligible, thus $\alpha_e^l(t)$ can be simply evaluated from the low-frequency wind fluctuations and static responses (Eq. (20)). In this case, the calculation of low-frequency response can be replaced by a static analysis at a given mean wind velocity. It is noted that nonlinearities in structural characteristics can also be readily incorporated into the analysis. For linear structures, modal analysis approach can be utilized to benefit from the reduction in computational effort afforded by limiting the number of modes.

6. Example

An example long-span suspension bridge with a main span of approximately 2000 m is used to investigate the effects of aerodynamic nonlinearities on flutter and buffeting responses. The equations in generalized modal coordinates consisting of the first 15 modes are used for describing the bridge motion. The logarithmic decrement for each mode is assumed to be 0.02. Only the wind forces acting on the bridge deck are considered here for simplicity and without loss of generality. The bridge deck has been discretized into 70 beam elements in the spanwise direction. The static force coefficients at varying angle of incidence are shown in Fig. 1. The flutter derivatives $H_1^* \sim H_4^*$ and $A_1^* \sim A_4^*$ are used for a twin-box section determined through wind tunnel testing at varying angle of incidence from -6° to 6° [12]. P_1^* is given based on the quasi-steady theory and others are neglected. For the sake of illustration, only the variation of A_2^* with angle of incidence is considered in the nonlinear analysis. Experimental data indicates that A_2^* is highly sensitive to the angle of incidence for

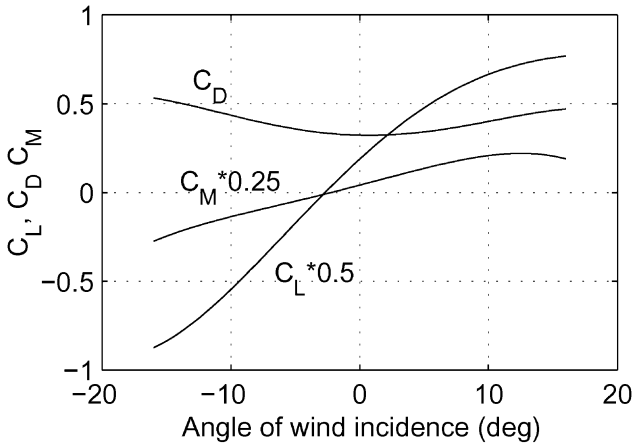

Fig. 1. Static force coefficients.

this section (Fig. 2). Since the experimental data is only available for several limited angles of incidence ranging from -6° to 6°, the values for other angles of incidence have been interpolated, and the values for the angles larger than 6° or less than -6° are assumed to remain constant at the values of 6° or -6°.

The nonlinearity of buffeting forces is introduced by the static force coefficients that are functions of angle of incidence as shown in Fig. 1. The admittance and the joint acceptance functions are considered not varying with the angle of incidence. The admittance functions used are given by Davenport's expression for drag, and Sears function for lift and pitching moment components. The spanwise correlation of buffeting forces is assumed to be the same as the corresponding wind fluctuations. The integral length scales and intensities used are 80 and 40 m, and 10% and 10%, for *u*- and *w*-components, respectively.

Fig. 3 shows the static torsional rotation of bridge deck along the bridge axis at varying mean wind velocities. It is noted that at high wind velocities the along-wind

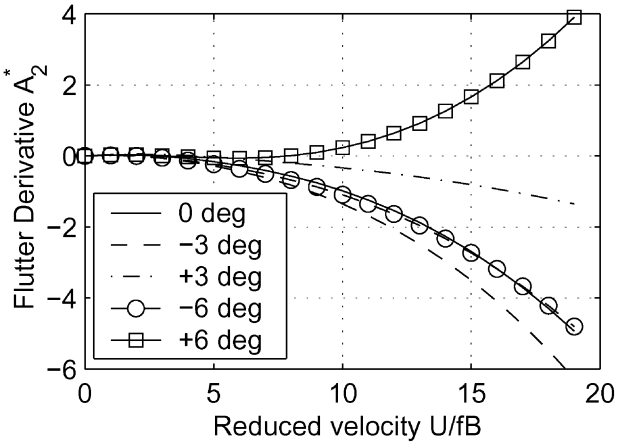

Fig. 2. Flutter derivative A_2^* at varying angles of incidence.

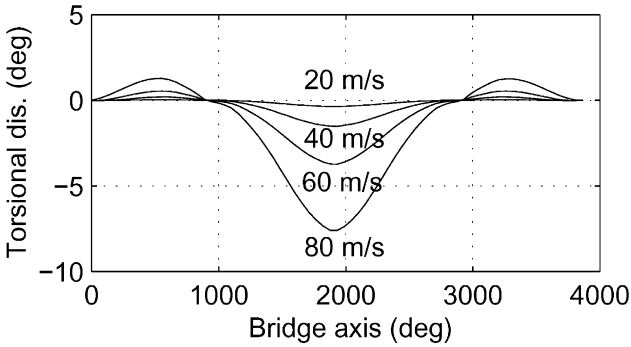

Fig. 3. Static deformation vs. mean wind velocity.

deformation is remarkable and the bridge deck show significant negative angle (nose-down) in torsion at the main span center.

The analysis of multimode coupled flutter in frequency domain is conducted by a complex eigenvalue analysis. Different natural mode combinations are considered which involve the first 15 natural modes, and a combination involving the first and second vertical bending and the first torsional mode (modes 2, 8, 10). Analysis in the time domain is also carried out by the simulation of the free vibration motion of the bridge [3].

Table 1 gives a comparison of the predicted critical flutter velocities. Results demonstrated the accuracy of the time domain scheme in predicting the flutter response. Figs. 4 and 5 show the variation of modal damping in mode 10 branch with wind velocity and the critical flutter velocity at varying mean wind angles of incidence. These are calculated using modes 2 , 8 and 10, and assuming that the angle of incidence is uniform in the spanwise direction. In Fig. 4, results of flutter analysis using self-excited forces linearized at the statically deformed position is also presented. Results indicate that the flutter response of this example bridge is very

Table 1
Critical flutter velocity (m/s)

Mode No.	$\alpha_e^l = 0$	$\alpha_e^l = \alpha_s$
(a) Frequency domain		
modes 2, 8, 10	72.1	74.1
modes 1–15	74.8	76.3
(b) Time domain		
modes 1–15	74.9	76.5

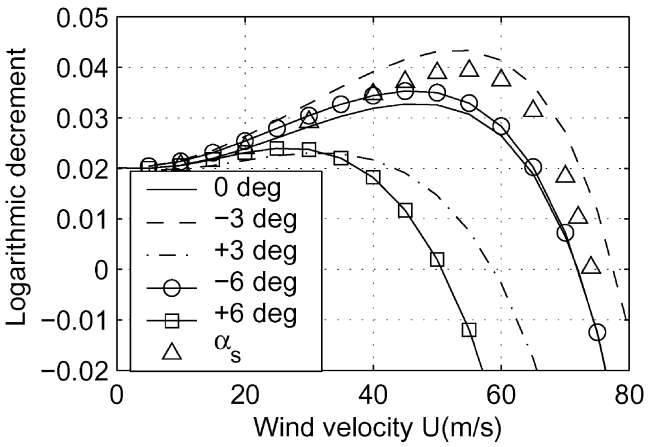

Fig. 4. Damping ratio vs. wind velocity.

sensitive to the angle of incidence of the mean wind velocity, particularly, for positive angles of incidence. Since the variation of flutter derivative A_2^* is insensitive to the negative angle of incidence, consideration of the static rotation of the bridge deck only slightly affects the flutter response for this example bridge. The wind fluctuations at the center of each element along bridge axis at a given wind velocity are simulated. A multi-variate correlated auto-regressive model is used to generate

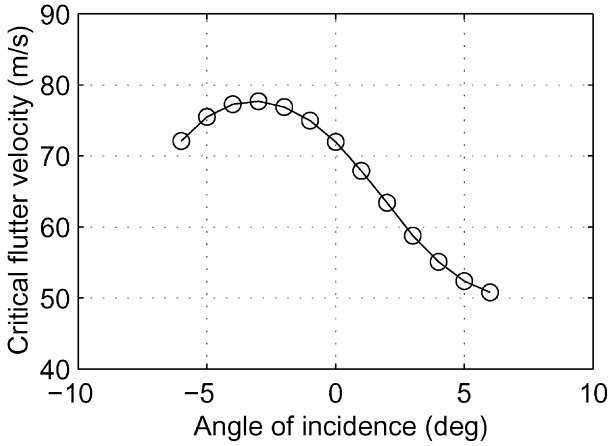

Fig. 5. Critical flutter velocity vs. angle of incidence.

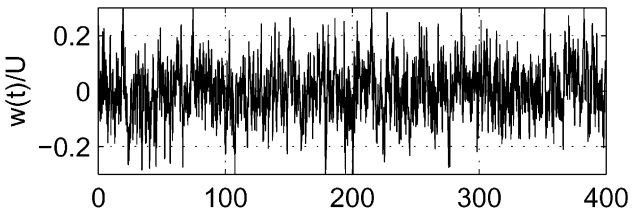

(a) Vertical wind fluctuation

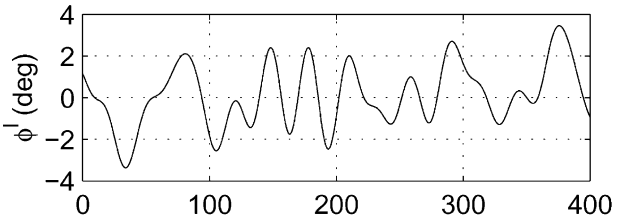

(b) Effective angle of incidence

Fig. 6. A realization of wind fluctuation and associated effective angle of incidence ($U = 60$ m/s): (a) vertical wind fluctuation, and (b) effective angle of incidence.

2400 s of time histories at increments of 0.1 s. An example realization of the vertical wind fluctuations at the center of the main span and associated effective angle of incidence calculated by its low-frequency component are shown in Fig. 6 at 60 m/s. Fig. 7 shows a comparison of the target power spectral density and those calculated based on simulated vertical wind fluctuations. Excellent agreement illustrated the accuracy of the simulation of wind fluctuations.

For comparison, both linear and nonlinear analysis are conducted at different mean wind velocity. In this example long-span bridge, the low-frequency component of the response is negligible, the effective angle of incidence at each element is

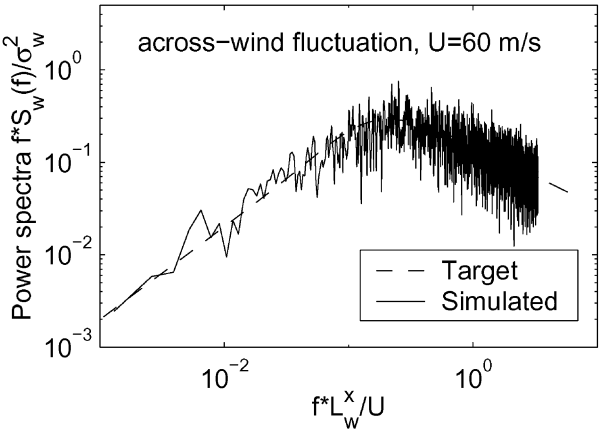

(a) original

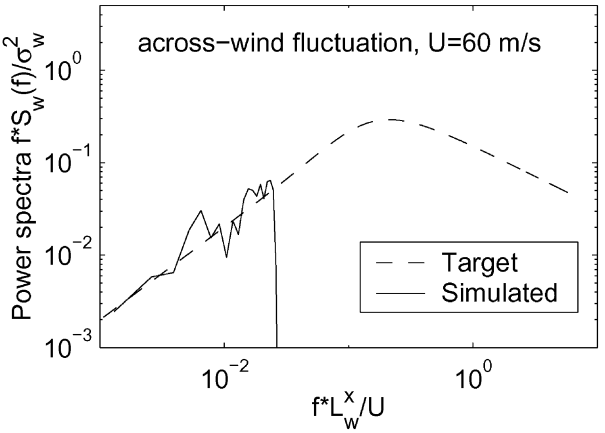

(b) Low-frequency component

Fig. 7. Comparison of the power spectral density of vertical wind fluctuation ($U = 60$ m/s): (a) original, and (b) low-frequency component.

calculated from the low-frequency wind fluctuations and the static rotation. Fig. 8 shows time history of the torsional rotation at the center of main span calculated by the nonlinear analyses at 60 m/s. Fig. 9 compares the root mean square (RMS) and maximum (MAX) torsional response of bridge deck along bridge axis at 60 m/s calculated by linear and nonlinear analysis. Fig. 10 is the time history of torsional rotation at the center of main span at 80 m/s at which the flutter initiates for both linear and nonlinear analysis with large amplitude of more than 10°.

It is noted that for this specific example the analysis based on nonlinear aerodynamic forces gives a slight higher response over the conventional linear approach. It is also noted that the aerodynamic stability of the bridge was reduced by the presence of the low-frequency turbulence as shown in Fig. 10. Similar result was also observed in Ref. [11]. The experimental observation of the changes in the critical flutter velocity due to turbulence also include the effects of changes in the flutter derivatives due to turbulence. This effect has not been included in this analysis, however, the procedure allows immediate application when the aerodynamic force parameters in turbulent flows become available.

For comparison, the analysis with mean wind angle of incidence of 3° and neglecting the contribution of static rotation to the effective angle of incidence is also conducted. Comparing with the former analysis in which the low-frequency effective

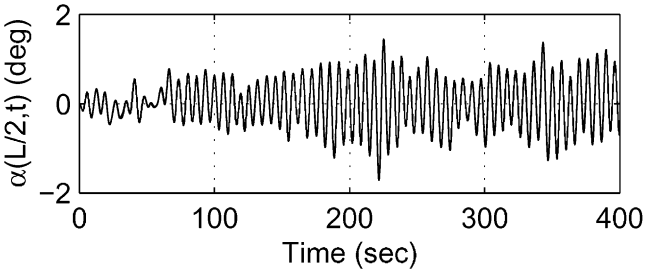

Fig. 8. Torsional rotation (nonlinear analysis, $U = 60$ m/s).

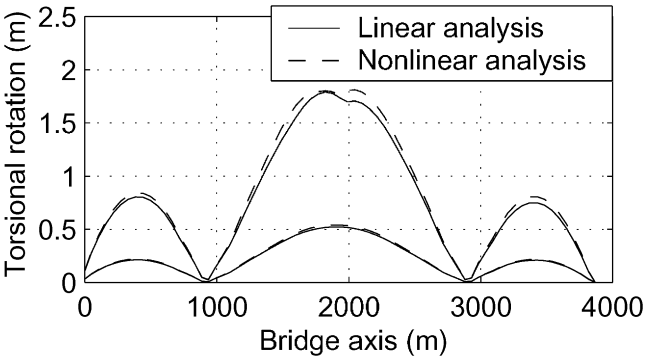

Fig. 9. Comparison of RMS and MAX torsional response ($U = 60$ m/s).

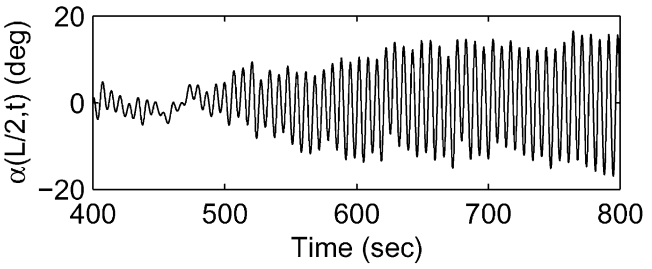

(a) Linear analysis

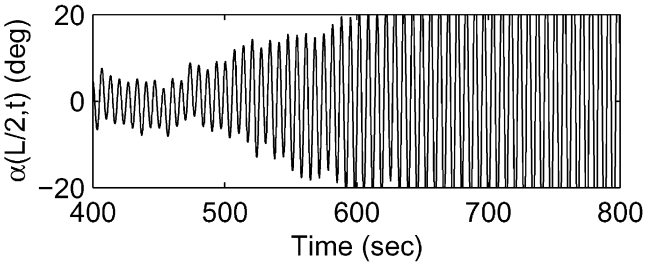

(b) Nonlinear analysis

Fig. 10. Torsional rotation ($U = 80$ m/s): (a) linear analysis, and (b) nonlinear analysis.

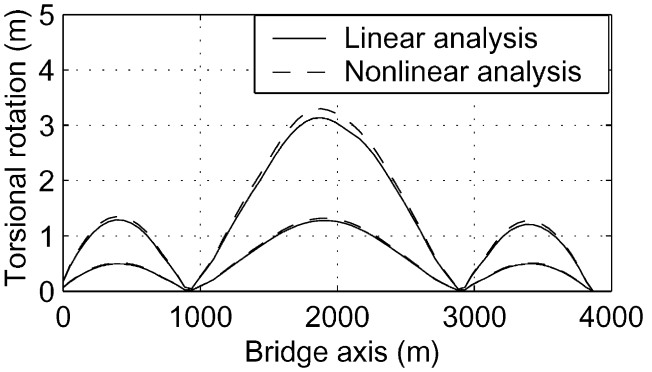

Fig. 11. Comparison of RMS and MAX torsional response ($U = 60$ m/s).

angle of incidence has a mean value of static rotation of the bridge sections, in this case the low-frequency effective angle of incidence has a mean value of 3°. From Figs. 4 and 5, it is noted that the modal damping of torsional motion dominated mode and flutter response are relatively sensitive to the changes in the angle of incidence within positive range. Fig. 11 shows the comparison of RMS and MAX torsional rotation obtained by linear and nonlinear analysis. The nonlinear analysis results in a higher response over the linear analysis. Compared with Fig. 9, it is seen that the buffeting response is very sensitive to the changes in the mean angle of incidence.

In this specific example, the result of nonlinear analysis does not show significant difference from the conventional linear analysis. This may be due to the fact that the modulation of force parameters with the instantaneous effective angle of incidence did not result in an apparent build up or decay of response. In addition, the modulation of the forces acting on different spanwise locations of the bridge deck cancelled one another such that the effect due to the changes in total forces on the bridge becomes less significant.

It is worth mentioning that the effects of the aerodynamic nonlinearity depend on the level of the effective angle of incidence and the sensitivity of the wind force parameters with respect to the effective angle of incidence. The results of this example bridge regarding the effects of nonlinear aerodynamics cannot simply be extended to other specific cases which require examination based on their aerodynamic and structural characteristics.

7. Concluding remarks

A time domain approach for predicting the buffeting and flutter responses with aerodynamic nonlinearities was presented. The nonlinear aerodynamic forces were modeled based on static force coefficients, flutter derivatives, admittance functions and their spanwise correlations at varying angles of incidence. A rational function approximation technique was utilized to involve the frequency dependent force parameters in time domain simulation.

Results of an example study indicated that the analysis involving the aerodynamic nonlinearity resulted in a slight higher response than the conventional linear analysis, and the low-frequency turbulence component has a destabilizing effect on the flutter instability. The effects of aerodynamic nonlinearity depend on the level of the effective angle of incidence and the sensitivity of the aerodynamic force characteristics with respect to the effective angle of incidence. Additional studies are needed to further advance our understanding of the effects of aerodynamic nonlinearities.

A coordinated experimental investigation is in progress for further validation of the proposed approach. This effort seeks an understanding of turbulence induced modifications in the magnitude and spanwise coherence of both the buffeting and the self-excited forces. Incorporating measurements of the effective angle and amplitude dependence of aerodynamic forces in the analysis framework will lead to a computational procedure for nonlinear analysis of long-span bridges. Furthermore, full aeroelastic bridge model tests will provide useful information for validating the proposed approach.

Acknowledgements

The support for this work was provided in part by NSF Grants CMS 9402196 and CMS 95-03779. This support is gratefully acknowledged.

References

[1] H. Katsuchi, N.P. Jones, R.H. Scanlan, Multimode coupled flutter and buffeting analysis of the Akashi-Kaikyo Bridge, J. Struct. Eng. ASCE 125 (1999) 60–70.
[2] X. Chen, M. Matsumoto, A. Kareem, Coupled flutter and buffeting response of bridges, J. Eng. Mech. ASCE 126 (1) (2000a) 17–26.
[3] X. Chen, M. Matsumoto, A. Kareem, Time domain flutter and buffeting response analysis of bridges, J. Eng. Mech. ASCE 126 (1) (2000b) 1–16.
[4] T. Miyata, H. Yamada, V. Boonyapinyo, J.C. Stantos, Analytical investigation on the response of a very long suspension bridge under gusty wind, Proceedings of the Ninth International Conference on Wind Engineering, ICWE, New Delhi, India, pp. 1006–1017.
[5] X. Chen, A. Kareem, Aerodynamic analysis of bridges under multi-correlated winds: integrated state-space approach, J. Eng. Mech. ASCE 127 (11) (2001) 1124–1134.
[6] Y. Nakamura, Bluff-body aerodynamics and turbulence, J. Wind Eng. Ind. Aero. 49 (1993) 65–78.
[7] M. Matsumoto, Recent study on bluff body aerodynamics and its mechanism, in: G.L. Larose, F.M. Livesey (Eds.), Wind Engineering into the 21 Century, Balkema, Rotterdam, 1999, pp. 67–78.
[8] Y.K. Lin, Q.C. Li, New stochastic theory for bridge stability in turbulent flow, J. Eng. Mech. ASCE 119 (1) (1993) 113–127.
[9] R.H. Scanlan, Amplitude and turbulence effects on bridge flutter derivatives, J. Struct. Eng. 123 (2) (1997) 232–236.
[10] F.L. Haan, The effects of turbulence on the aerodynamics of long-span bridges, A dissertation submitted to the Graduate School of the University of Notre Dame, In partial fulfillment of the requirements of the Degree of Doctor of Philosophy, 2000.
[11] G. Diana, F. Cheli, A. Zasso, M. Bocciolone, Suspension bridge response to turbulent wind: comparison of new numerical simulation method results with full scale data, in: G.L. Larose, F.M. Livesey (Eds.), Wind Engineering into the 21 Century, Balkema, Rotterdam, 1999, pp. 871–878.
[12] M. Matsumoto, T. Yagi, H. Ishizaki, H. Shirato, X. Chen, Aerodynamic stability of 2-edge girders for cable-stayed bridge, Proceedings of 15th National Symposium on Wind Engineering JAWE, 1998, pp. 389–394 (in Japanese).
[13] R.H. Scanlan, Problematics in formulation of wind-force models for bridge decks, J. Eng. Mech. ASCE 119 (7) (1992) 1353–1375.
[14] M.S. Li, D.X. He, Aerodynamic admittance of bridge deck sections, Proceedings of the Second European & African Conference on Wind Eng. (2EACWE), Genova, Italy, 1997, pp. 1585–1592.
[15] K. Wilde, Y. Fujino, J. Masukawa, Time domain modeling of bridge deck flutter, J. Struct. Mech. Earthquake Eng. JSCE 13 (2) (1996) 93–104.
[16] A. Kareem, Analysis and modeling of wind effects: numerical technique, in: G.L. Larose, F.M. Livesey (Eds.), Wind Engineering into the 21 Century, Balkema, Rotterdam, 1999, pp. 43–54.